TOMOGRAPHIC RECONSTRUCTION OF THE LONGITUDINAL DISTRIBUTION FUNCTION OF IONS IN BUNCHES DURING ACCELERATION AT THE NUCLOTRON

V. M. Zhabitsky*, Joint Institute for Nuclear Research, Dubna, Russia

Abstract

Methods of processing a digital signal proportional to the longitudinal intensity of ions in bunches during their acceleration in synchrotrons are discussed. The method of computerized tomography is used for reconstruction a longitudinal two-dimensional distribution function of ions in the bunch from the data on its profiles depending on synchrotron motion of particles. Examples of tomographic studies of ion beams at the Nuclotron are presented.

INTRODUCTION

Methods of computerized tomography — mathematical algorithms for reconstruction of the internal structure of an object from the collection of projection data — are widely used in modern scientific research. Typically, projection data are obtained for a thin layer (cross-section of the object), the internal structure of which is described by a two-dimensional distribution function. A bunch of charged particles circulating along the orbit of the synchrotron and performing longitudinal (synchrotron) oscillations with respect to the synchronous particle [1] can be included to the class of tomographic objects. Indeed [2, 3], let $s_0(t)$ be the displacement of a synchronous particle with energy E_0 along the orbit relative to the accelerating section at time instant t. Then the longitudinal distribution function $f(E - E_0, s - s_0)$ of charged particles in the bunch occupying the position s and having energy E depends on deviations $E - E_0$ and $s - s_0$. The one-dimensional distribution function, which is a two-dimensional projection of the function $f(E - E_0, s - s_0)$ on the time axis coincides with the longitudinal intensity profile of the bunch $n(t)$ – the number of particles distributed in the bunch, as measured by the sensor of the pulse current. The analog signal $n(t)$ is usually converted into a sequence of digital samples $n[i]$ corresponding to the time instants $t_i = i \cdot T_{\rm clk}$ with a constant sampling period $T_{\rm clk}$.

The methods presented in [4] provide digital processing of the $n[i]$ signal generated by a proton bunch in the synchrotron CERN PSB in order to reconstruct the two-dimensional longitudinal distribution function of particles in the bunch. Methods of data recording and their subsequent processing in order to reconstruct the longitudinal two-dimensional ion distribution function in an accelerated bunch at the Nuclotron [5] are described followed.

BASIC PROCEDURE

It was demonstrated in [4] that the procedure of computerized tomography for bunches of charged particles in a synchrotron allows to reconstruct two-dimensional longitudinal distribution function of particles in the bunch, making synchrotron oscillations. The phase trajectories of particles with small deviations from the synchronous one are closed under the conditions of the phase stability principle and surround a stable equilibrium point $\phi = \phi_s$. The impulse function $n(t)$ at each revolution is a projection of the bunch phase portrait on the time axis. To identify a set of digital sequences for bunch intensity profiles, a specialized digital device was used in [4] which allowed to synchronize the measurement process (see Fig. 1 and paper [3]) with accelerating voltage $\tilde{V}_{\rm rf}(t)$.

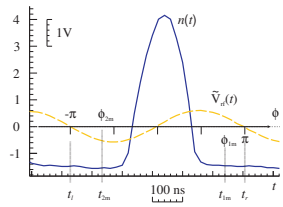

Figure 1: Graphs for $n(t)$ and accelerating voltage $\tilde{V}_{\rm rf}(t)$

As a result, a sequence of digital functions $f_j[i, j, k]$ was formed on each revolution of k for the bunch with the number j, which are a characteristic of the differential law of particle distribution by the slot i within the bunch with the number j on the turn k with the starting point $t_l = t_i(\phi_j[k] = -\pi)$. The set of these intensity profile data was used in the computational tomography procedure [4], where the **a**lgebraic **r**econstruction **t**echnique (ART) was used [6, 7]. Additional parameters of the computational algorithm in the given time of reconstruction of $t = t_{\rm init}$ for accelerating charged particles with rest mass m and charge q that circulates along the equilibrium orbit with average radius R_0 are the guide magnetic induction $B(t)$ and the speed of its changes in time $\dot{B}(t)$, the amplitude of the accelerating voltage on the gap $V(t)$ and speed of its change in time $\dot{V}(t)$, the rf harmonic number $h_{\rm rf}$, the transition gamma $\gamma_{\rm tr}$, the bending radius ρ.

The functional scheme of registration of data on the intensity of bunches for the purpose of tomographic studies at the Nuclotron was described in [3] and is shown in Fig. 2. Five equidistant bunches ($h_{\rm rf} = 5$) circulate along the orbit in the Nuclotron. The intensity of bunches is observed by the pick-up, the signal from which is available for users. The analog signal from the pick-up $n(t)$ goes to the two-channel digitizer ($T_{\rm clk} = 10$ ns). The second input of the digitizer is fed by the harmonic signal from accelerating section $\tilde{V}_{\rm rf}(t) = V_0 + V(t)\cos(\omega_{\rm rf}(t) + \varphi_0)$. The angular frequency $\omega_{\rm rf}(t)$ is determined in accordance with the law of change of the magnetic induction in dipoles $B(t)$. As a result,

* V.Zhabitsky@jinr.ru

ISBN 978-3-95450-197-7

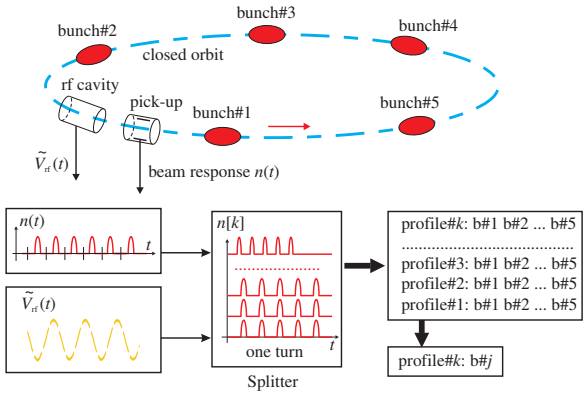

Figure 2: Functional data logging scheme.

two digital signals $n[i]$ and $\tilde{V}_{\rm rf}[i]$ are generated, which are transmitted to a remote computer, where all the necessary signal processing and computed tomography procedures are performed. First, the joint processing of these digital signals is carried out in order to convert a one-dimensional data array $n[i]$ into a three-dimensional data array on i inside the bunch with the number j at the turn k by the **Splitter** procedure. Then, the procedures are performed to convert the three-dimensional data array into projection data $f[i,j,k]$ for $h_{\rm rf}$ bunches required for the tomographic procedure starting at $t_{\rm init}$. Finally, the profile data $f_j[i,j,k]$ of a particular bunch j is performed for the computed tomography procedure. To reduce noise and eliminate the base level shift, the *phase selection* procedure [3] is performed by gating the detected signal for the duration of the part of the signal that is caused by particles in the accelerated bunch inside separatrix. Therefore, the profile data $f_j[i,j,k]$ correspond to the finite positive function and can be used in the ART.

It should be emphasized that the **Splitter** procedure sets the length of the array on i in accordance with the maximum period $T_{\rm rev}$ of circulated particles. Since the period $T_{\rm rev}$ decreases at acceleration, for the array $f_j[i,j,k]$ only the initial points correspond to the intensity of the bunches. When $t(k) > T_{\rm rev}(k)$ the elements of the array on i at the k-turn are the same as the value of its first element (see Fig. 2).

The described procedure of transition from the digital signal $n[i]$ for the pulse intensity of circulating bunches to the functions $f_j[i,j,k]$, which are characteristic of the differential law of particle distribution in the bunch j on the turn k, allows to reveal the projection data necessary for the algorithm of computed tomography at each turn. The correctness of this procedure is controlled visually by constructing a three-dimensional graph for intensity profiles. In this case, the value of the digital signal delay $\tilde{V}_{\rm rf}[i]$ is selected so that all profiles for $n[i]$ follow each other consistently.

Example of the three-dimensional graph for intensity profiles for deuteron beam in the Nuclotron is shown in Fig. 3 (the number k of turns recoded during 50 ms is 7653). Result [3] of tomographic reconstruction of the longitudinal distribution function of deuterons is shown in Fig. 4.

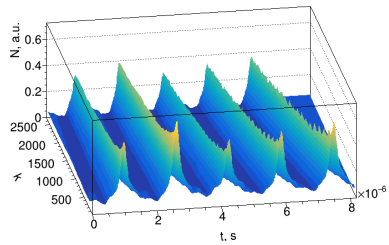

Figure 3: 3D graph for intensity profiles.

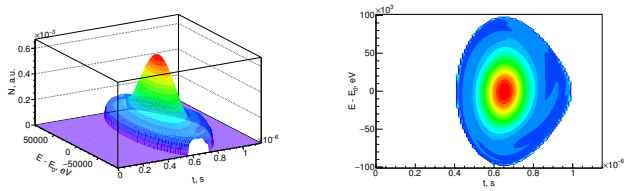

Figure 4: Tomogram (3D on left, 2D on right).

The time interval $t \in [42\,\text{ms}, 47\,\text{ms}]$ for reconstruction was chosen in accordance with the conditions given in [4] when $\dot{B}(t) = \text{const}$ and $V(t) = \text{const}$.

IMPROVED PROCEDURE

It is clear that fragment of the recorded data was used to obtain Fig. 4. A tomographic reconstruction procedure for application in a wider time interval with an arbitrary dependencies $B(t)$ and $V(t)$ on time t is described followed.

Theoretical Model

Piecewise-defined functions without jumps of its first and second derivatives are used for definition of $B(t)$ and $V(t)$ approximated by N-degree polynomials **polN** [8]. So, graph in Fig. 5a for $B(t)$ is combined using **pol0** (injection plateau), **pol4**, **pol1** (linear ramp), **pol4**, **pol0** (top energy plateau).

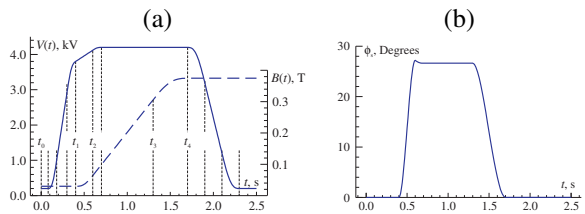

Figure 5: (a) $B(t)$ (dashed) and $V(t)$ (solid). (b) $\phi_{\rm s}$

The same approach is used for $V(t)$ taking into account $B(t)$ dependence. Resulting graph for synchronous phase $\phi_{\rm s}$ is shown in Fig. 5b.

To set up the ART application, coordinated with the projection data, the following model was used [3]. As the first step, the initial two-dimensional function of the longitudinal distribution of test particles within the separatrix for a single bunch at the given time instant was specified. Then, for the magnetic induction $B(t)$ and the rf voltage with the amplitude $V(t)$ consistent with $B(t)$, the difference equations [1] for synchrotron oscillations were used to determine changes

ISBN 978-3-95450-197-7

in the position of test particles on the phase plane during their rotation within the separatrix along phase trajectories and the projections of an arising instantaneous two-dimensional distribution function onto the time axis were calculated at each turn. For the initial distribution function, a superposition of two functions, corresponding to the normal particle distribution (Gaussian function) in phases and energies, was used. The centre of the first distribution function was displaced in energy by a positive value with respect to the synchronous particle, while the centre of the second function was displaced by a negative value; here the narrower distribution function was used for it. This leads to coherent longitudinal oscillations of particles in the bunch, which can be seen on the plot for intensity profiles. The data thus obtained for intensity profiles correspond to the finite positive function, which has nonzero values only inside the separatrix. Consequently, they can be utilized to reconstruct the two-dimensional particle distribution function in the bunch using the ART.

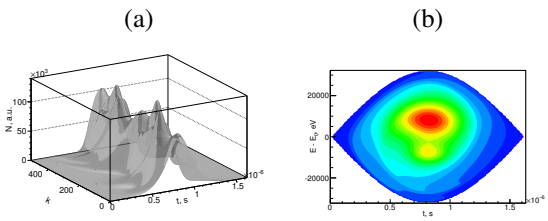

Figure 6: (a) Bunch profiles. (b) Tomogram.

The theoretical model was successfully used in [3] in the framework of basic procedure (linear dependencies of $B(t)$ and $V(t)$ on time t). Thus, bunch profiles on injection plateau ($\phi_s = 0$) are shown in Fig. 6a. Tomogram plot is shown in Fig. 6b.

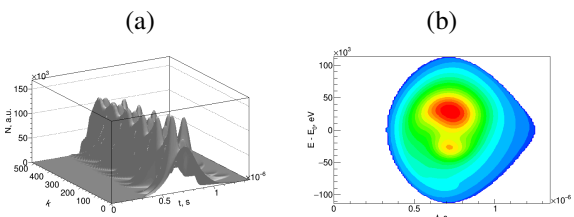

Figure 7: (a) Bunch profiles. (b) Tomogram.

Tomographic reconstruction technique improved by author for more complex dependencies of $B(t)$ and $V(t)$ on time was tested successfully too. Results at $\phi_s = 11.4°$ (see Fig. 5) are shown in Fig. 7. Displacements on tomogram plot in particle energies and differences in values of dispersions correspond to the initial distribution functions.

EXPERIMENTAL RESULTS

The first example discussed concerns acceleration of carbon ions C^{6+} during the run 55 at the Nuclotron in March 2018. Short pulse of ions was injected into the Nuclotron. Thus, only bunch #4 was captured and accelerated. Plots for its evolution are shown in Fig 8. Ions made 554640 turns during 800 ms (Fig 8a). The graph after injection is shown in Fig 8b (2452 turns in 20 ms).

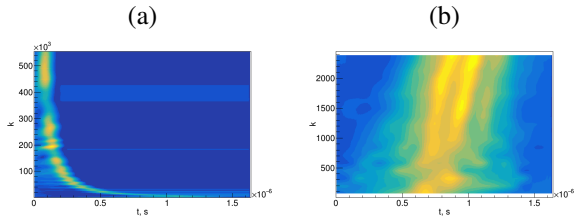

Figure 8: Bunch #4 plots during 800 ms (a) and 20 ms (b).

In order to use the tomographic reconstruction technique for experimental data of profiles it is necessary to define, first of all, $B(t)$ and $\dot{B}(t)$ functions. The method described above and in [2, 3, 9] allows to calculate $B(t)$ from $f_{\mathrm{rev}}(t)$ because starting points $t_l = t_i(\phi_j[k] = -\pi)$ are calculated for all rf periods (see Fig 1). These experimental data for $B(t)$ can be fitted by a set of polynomials taking into account general conditions for $B(t)$ namely the beam is injected on the plateau of magnetic field (**pol0**, starting point $t_{\mathrm{l}1} = t_{\mathrm{inj}}$) and accelerated further during its ramp (**pol1**, final point $t_{\mathrm{r}k} = 0.8$ s, see Fig. 9a). Time interval for **pol0** from $t_{\mathrm{l}1}$ to $t_{\mathrm{r}1}$ is set approximately from graph $B(t)$. The next time intervals for **pol4** are set approximately from graph $B(t)$ too. The last time interval for **pol1** is set approximately from graph $B(t)$ in the region of the linear dependence of $B(t)$ on time from $t_{\mathrm{l}k} = 0.5$ s till $t_{\mathrm{r}k} = 0.8$ s. After this draft initialization of time intervals for polynomials the standard procedure for crosslinking of polynomials in intervals located in the region of $(t_{\mathrm{r}m}, t_{\mathrm{l}(m+1)})$ is calculated. The crosslinking procedure is considered successful if for new calculated points $t_{\mathrm{r}m}$ and $t_{\mathrm{l}(m+1)}$ the condition $|t_{\mathrm{r}m} - t_{\mathrm{l}(m+1)}| < \Delta t_{\mathrm{ac}}$ is true with a given accuracy Δt_{ac}. In unsuccessful case an additional polynomial **pol4** is inserted and the crosslinking procedure is repeated.

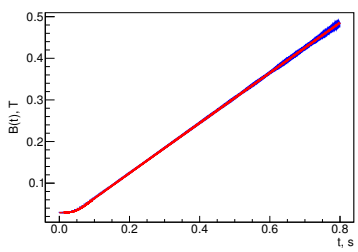

$B(t)$	t_{l}, ms
pol0	0.002
pol4	9.000
pol4	13.593
pol4	64.704
pol4	94.504
pol4	381.104
pol1	552.389

Figure 9: (a) Experimental data for $B(t)$ calculated from $f_{\mathrm{rev}}(t)$ (blue line) and its B-fitting (red line) by polynomials in accordance with data in table (b).

So, five **pol4** polynomials (see data table in Fig. 9b) are sufficient for $B(t)$ shown in Fig. 9a with accuracy $\Delta t_{\mathrm{ac}} = 1$ μs. Therefore, B-fitting procedure can be used for determination of $B(t)$ and $\dot{B}(t)$ functions.

The same procedure can be used for the rf voltage dependence $V(t)$. Unfortunately $V(t)$ data are not available to

ISBN 978-3-95450-197-7

remote reading at present. But the time interval of rising $V(t)$ and its speed are known. Thus, the voltage increase from 300 V to 6 kV was about 30 ms in run 55.

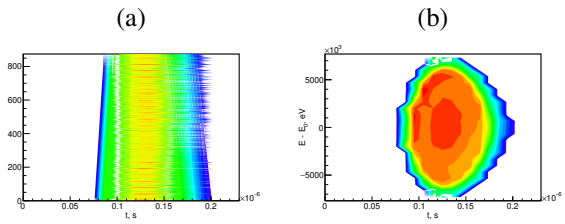

Figure 10: (a) Profiles of b#1. (b) Tomogram.

Therefore, tomographic reconstruction procedure can be tested, for example, at starting point $t_{\text{init}} = 500$ ms. Profiles of bunch #1 are shown in Fig. 10a. Reconstructed longitudinal distribution function is shown in Fig. 10b.

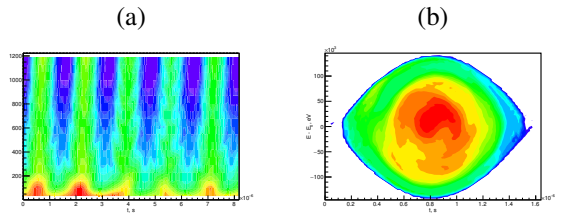

Figure 11: (a) Profiles of b#1 - b#5. (b) Tomogram of b#1.

The second example discussed concerns acceleration of lithium ions Li^{3+} during the run 54 at the Nuclotron in March 2017. Ions injected are bunched after 5 ms (see Fig. 11a). Reconstructed longitudinal distribution function is shown in Fig. 11b.

CONCLUSION

Tomographic reconstruction of the longitudinal distribution function of ions in bunches during acceleration was successfully tested at the Nuclotron. The technique of B-fitting on the basis of experimental data on rf frequency was developed. Tomographic reconstruction procedure was improved for an arbitrary dependencies of $B(t)$ and $V(t)$ on time t. Computed procedure developed can be used for estimation of longitudinal parameters of ion bunches.

ACKNOWLEDGEMENTS

I am grateful to A. Butenko, E. Gorbachev, S. Romanov, O. Brovko, A. Grebentsov, V. Karpinsky, B. Vasilishin, V. Andreev, V. Slepnev (JINR) for fruitful discussions and assistance in obtaining experimental data at the Nuclotron.

REFERENCES

[1] Handbook of Accelerator Physics and Engineering, Ed. by A. Chao, M. Tinger. Singapore: World Scientific, 1999. 740 p.

[2] V. M. Zhabitsky. Digital Methods for Diagnostics of Longitudinal Bunch Parameters in Synchrotrons. Physics of Particles and Nuclei Letters. 2016. Vol. 13, No.1. Pp. 127–131.

[3] V. M. Zhabitsky. Tomography of the Ion Bunches at the Nuclotron. Physics of Particles and Nuclei Letters. 2018. Vol. 18, No.7. Pp. 757–763.

[4] S. Hancock, P. Knaus, M. Lindroos. Tomographic Measurements of Longitudinal Phase Space Density. Proc. of the Sixth European Particle Accelerator Conference, 22–26 June 1998, Stockholm, Sweden. Institute of Physics. JACoW.org, 1998. Pp. 1520–1522. CERN–PS–98–030–RF, Geneva, 1998.

[5] A. Sidorin, N. Agapov, A. Alfeev et al. Status of the Nuclotron. Proc. of XXV Russian Particle Accelerators Conference RuPAC-2016, 21–25 November 2016, St. Petersburg, Russia. Saint Petersburg State University. JACoW.org, 2016. Pp. 150–152.

[6] R. Gordon. A Tutorial on ART. IEEE Transactions on Nuclear Science. June 1974. Vol. NS-21(3). Pp. 78–93.

[7] G. T. Herman. Image Reconstruction from Projections. The Fundamentals of Computerized Tomography. New York - London. Academic Press, 1980. 316 p.

[8] P. Cheblakov, A. Derbenev, R. Kadyrov et al. NSLS-II Booster Ramp Handling. Proc. of the 14th International Conference on Accelerator & Large Experimental Physics Control Systems ICALEPCS2013, 6–11 October 2013, San Francisco, USA. NIF/LLNL, JACoW.org, 2013. Pp. 1189–1192.

[9] V. M. Zhabitsky. Methods of Computer Processing of Experimental Data on the Intensity of Bunches in Synchrotrons. Physics of Particles and Nuclei Letters. 2016. Vol. 13, No.7. Pp. 829–832.

ISBN 978-3-95450-197-7